

Final Report
Date of Submission of Report: February, 2022

**Federal Agency/
Organization Element:** DOE/EERE/ Office of Advanced Manufacturing Program
(AMO)

Award Number: DE-EE0007254

Project Title: Fully Integrated High Speed Megawatt Class Motor and High
Frequency Variable Speed Drive System

Project Period: May 1, 2016 to October 31, 2021

Recipient Organization: Clemson University
Office of Sponsored Programs
300 Brackett Hall
Box 345702
Clemson, South Carolina, 29634-5702

DUNS Number: 04-262-9816

Principal Investigator: Ramtin Hadidi, (843) 730-5106, rhadidi@clemson.edu

Business Contact: Marlyn Grant, (864) 656-3592, marlyng@clemson.edu

Partners: **TECO Westinghouse Motor Company**
Haran Karmaker,
karmakeh@tecowestinghouse.com

DOE Technology Manager: Albert Hefner Jr., allen.hefner@nist.gov

DOE Project Officer/Manager: Debbie Schultheis, 720-356-1811,
debbie.schultheis@ee.doe.gov

DOE Project Monitor: Genny Fultz, 765-418-1845, genny.fultz@ee.doe.gov

DOE Award Administrator: Chris Kudola, 720-356-1675, chris.kudola@ee.doe.gov

Submitting Official: Ramtin Hadidi, Assistant Professor,
(843) 730-5106, rhadidi@clemson.edu

Acknowledgement: This material is based upon work supported by the U.S. Department of Energy's Office of Energy Efficiency and Renewable Energy (EERE) under the Advanced Manufacturing Office Award Number DE-EE0007254.

Disclaimer: This report was prepared as an account of work sponsored by an agency of the United States Government. Neither the United States Government nor any agency thereof, nor any of their employees, makes any warranty, express or implied, or assumes any legal liability or responsibility for the accuracy, completeness, or usefulness of any information, apparatus, product, or process disclosed, or represents that its use would not infringe privately owned rights. Reference herein to any specific commercial product, process, or service by trade name, trademark, manufacturer, or otherwise does not necessarily constitute or imply its endorsement, recommendation, or favoring by the United States Government or any agency thereof. The views and opinions of authors expressed herein do not necessarily state or reflect those of the United States Government or any agency thereof.

Final Report

Fully Integrated High Speed Megawatt Class Motor and High Frequency Variable Speed Drive System

Project Period:

Start Date: 5/1/2016

Completion Date: 10/31/2021

Project Team

Clemson University
Curtiss Fox, Jesse Leonard, Ramtin Hadidi, Thomas Salem
TECO Westinghouse Motor Company
Haran Karmaker, James Keck, Edward Chen, Enrique Ledezma, Paulo Guedes-Pinto, John Hu

February 28, 2022



Executive Summary

This project involved developing a fully integrated high speed megawatt class motor and high frequency variable speed drive system that serve as a commercially viable and technically sound methodology for high speed industrial system applications. The partnering organizations for this project formed an academic and industrial collaboration that combines the design, analysis, manufacturing and testing experience required for a large research project of this magnitude. The proposed project team organizations consist of Clemson University and TECO Westinghouse Motor Company (TWMC).

Based on extensive experiences in electric machines development, a preliminary baseline squirrel cage induction motor design has been prepared for the ratings of the FOA. The project teams have identified many improvements carried out during the initial phase of the proposed program to make it a commercially viable product including the use of low-loss steel laminations and Litz wire conductors for the stator coils. The baseline motor design has been further developed considering mechanical and thermal design concepts to contain high rotational stress and to minimize the losses to achieve the technical targets of the FOA. Rotor dynamics analysis has been thoroughly performed using modern multi-physics commercial software. Thermal management has been investigated by using computational fluid dynamics analysis software. Special manufacturing tools have been developed to perform trade-off studies to evaluate the costs and feasibility of the new system.

The proposed drive technology is the series-connected H-bridge (SCHB) topology which has been thoroughly studied and tested at megawatt levels by the research teams. By series connection of the inverter H-bridge cells, this topology has proven to have unique properties of handily matching medium-voltage applications while operating with low power losses at high switching frequency. Commercially available wide band gap (WBG) semiconductors have been incorporated into the SCHB topology to reach the required switching frequencies and efficiencies.

The project resulted in an integrated high speed megawatt class medium voltage motor drive system that is at a TRL 6 with a clear path for commercialization. The fully integrated prototype system has been manufactured by TWMC in its Round Rock, Texas facility and tested at full power on a dynamometer at the Clemson University's eGRID Center in North Charleston, South Carolina.

Table of Contents

1. INTRODUCTION	1
2. MEDIUM VOLTAGE POWER CONVERTER	1
3. HIGH SPEED INDUCTION MACHINE.....	4
4. FULLY INTEGRATED SYSTEM VALIDATION.....	9
5. OTHER PRODUCT	13
5.1. PATENTS	13
5.2. PAPERS.....	14
5.3. PRESENTATIONS	14
5.4. REPORTS	14
6. IMPACTS.....	14
7. REFERENCES	15

Table of Tables

TABLE 1: HIGH FREQUENCY CONVERTER SPECIFICATIONS: HYBRID SiC SYSTEM TOPOLOGY	4
TABLE 2: HIGH-SPEED INDUCTION MACHINE SPECIFICATIONS	5
TABLE 3: FULL RATED POWER MOTORING HEAT RUN RESULTS.....	10
TABLE 4: HALF RATED POWER MOTORING HEAT RUN RESULTS	10
TABLE 5: THD FOR INPUT AND OUTPUT DRIVE VOLTAGE AND CURRENT FOR 100% POWER TEST.	13

Table of Figures

FIGURE 1: THE GENERAL STRUCTURE OF THE SERIES CONNECTED FULL SiC H-BRIDGE TOPOLOGY.	2
FIGURE 2: MEASUREMENTS AND HARMONIC ANALYSIS OF THE SCHB TOPOLOGY WITH A 4160V 60 HZ OUTPUT VOLTAGE SWITCHING AT 2 KHz; (A) SCOPE CAPTURE OF THE OUTPUT LINE TO LINE VOLTAGE AND (B) THE PERCENT OUTPUT VOLTAGE THD CALCULATIONS FOR THE FIRST 500TH HARMONICS.	2
FIGURE 3: (A) THERMAL IMAGING OF THE HYBRID POWER CUBE UNDERGOING INITIAL FULL LOAD TESTING AND (B) THE WAVEFORMS FROM THE SAME HYBRID POWER CUBE SHOWING ON THE TOP THE 500 HZ OUTPUT VOLTAGE AND CURRENTS AND ON THE BOTTOM, THE VOLTAGE AND CURRENT OF ONE PHASE OF THE THREE PHASE ACTIVE RECTIFIER.	3
FIGURE 4: (A) BENCHTOP TESTING OF THE FULL SiC POWER CUBE AND (B) THE ASSEMBLY OF THE SiC MOSFET, GATE DRIVER BOARD AND FIBER OPTIC GATE DRIVER INTERFACE (FGDI) BOARD USED IN THE FULL SiC POWER CUBE DESIGN.	4
FIGURE 5: THE PROTOTYPE HIGH SPEED INDUCTION MACHINE WITH A FLANGED SHAFT PREPARED FOR FACTORY ACCEPTANCE TESTS.	5
FIGURE 6: LITZ WIRE COIL SAMPLE, STATOR WITH LITZ WIRE AND LITZ WIRE JOINT TESTS.	6
FIGURE 7: (A) THE BENCHTOP TESTER FOR THE LITZ WIRE COILS, (B) THE ELECTROMAGNETIC SIMULATION MODEL OF THE LITZ WIRE TESTER AND (C) THE RATIO OF THE AC RESISTANCE TO THE DC RESISTANCE UP TO 50 KHz.	6
FIGURE 8: BODE PLOT (LEFT) AND ROTOR AND BEARING PROFILE (RIGHT) USED FOR THE ROTOR DYNAMIC DESIGN AND ANALYSIS USED IN THE HIGH SPEED INDUCTION MACHINE DESIGN.	7
FIGURE 9: (A) FEA ANALYSIS OF ROTOR GROOVING SURFACE TREATMENT TO REDUCE EDDY CURRENT LOSSES ON THE INDUCTION MACHINE ROTOR SHOWN IN (B) DUE TO SLOT HARMONICS CAUSED BY THE STATOR.	8
FIGURE 10: THE BURST TEST ROTOR WITH COPPER BARS FOR HIGHER EFFICIENCY AND GROOVES TO LOWER SURFACE EDDY CURRENTS. (A) COMPLETE ROTOR AFTER 25% OVER SPEED TEST, (B) LOWER ROTOR END RINGS SHOWING NO ISSUES, AND (C) UPPER ROTOR END RINGS SHOWING SOME BAR MOVEMENT DUE TO UNRELIABLE TORCH BRAZING THAT WAS CORRECTED WITH INDUCTION BRAZING IN THE FINAL ROTOR.	8
FIGURE 11: FEA THERMAL ANALYSIS OF THE INDUCTION MACHINE FOR FORCED AIR COOLING WITH A FLOW RATE OF 2400 CFM OF THE (A) FULL INDUCTION MACHINE MODEL, (B) STATOR CORE, AND (C) ROTOR.	9
FIGURE 12: THE HIGH-SPEED DYNAMOMETER TEST SETUP FOR SYSTEM VALIDATION AT THE CLEMSON UNIVERSITY EGRID CENTER.	10
FIGURE 13: 100% POWER HEAT RUN DATA: HIGH SPEED MACHINE TORQUE, SPEED, VIBRATION AND WINDING TEMPERATURES.	11
FIGURE 14: 100% POWER HEAT RUN DATA: HIGH SPEED MACHINE COOLING SYSTEM DATA.	11
FIGURE 15: INPUT AND OUTPUT VOLTAGE AND CURRENT WAVEFORM FOR 100% POWER HEAT RUN.	12
FIGURE 16: OUTPUT HARMONICS DATA FOR 100% POWER HEAT RUN.	12
FIGURE 17: INPUT HARMONICS DATA FOR 100% POWER HEAT RUN.	13

1. Introduction

This project involved developing a fully integrated high speed megawatt class motor and high frequency variable speed drive system that serve as a commercially viable and technically sound methodology for high speed industrial system applications. The partnering organizations for this project formed an academic and industrial collaboration that combines the design, analysis, manufacturing and testing experience required for a large research project of this magnitude.

The project team developed design concepts and manufactured a fully integrated high speed motor and drive prototype system with an emphasis on power density and overall system efficiency. The integrated system has been comprehensively tested and validated in order to reach Technology Readiness Level (TRL) of 6. The project enhanced manufacturing capabilities within the United States by developing innovative processes and systems. The project partners developed a commercialization plan that focus on reducing the installed cost of the system and aid in tailoring the system for specific industries and applications

2. Medium Voltage Power Converter

The current state-of-the-art in medium voltage power converters is trending towards using higher voltages in traditional power converter topologies. In a traditional medium-voltage drive design, this results in the requirement that the semiconductor devices be able to block higher voltages. Although this is possible with Wide-Bandgap (WBG) semiconductor devices, the practicality of switching higher voltages with fast switching times leads to an increase in switching noise and special motor winding insulation requirements. However, to achieve high frequency operation, WBG semiconductor devices are required to achieve practical efficiencies.

To overcome these challenges, the variable frequency high-speed drive utilizes an advanced series-connected H-bridge (SCHB) inverter topology that is suitable for both medium voltage and high frequency output [1]. In the SCHB design, the voltage across the individual WBG device is lower leading to a more practical implementation of both the motor and the drive, especially with today's commercially available WBG semiconductors. Additionally, the variable frequency high speed drive leverages the experience and effort obtained from the design and construction of a similar topology based upon Si semiconductors.

Two power cube converter topologies were developed for this project. The first "hybrid SiC converter topology" integrates Si IGBT active front end (AFE) input stage, and SiC MOSFETs H-bridge (HB) output stage. The second "full SiC converter topology" is built with both AFE and HB power stages using SiC MOSFETs. The hybrid SiC system targets medium voltage applications where the overall system cost will be kept low. The full SiC converter topology is preferred where system efficiency and high performance are the key design factors. Both medium voltage SiC based converter constructions result in multilevel SCHB inverter topologies.

Figure 1 is depicting the full SiC SCHB topology. Each multi-level phase output is generated by a set of isolated H-bridges connected in series to yield a phase output voltage equal to the sum of the individual H-bridges. Galvanic isolation of the individual H-bridges is provided through integrated medium voltage step-down transformers and careful isolation design within the drive cabinets is required. The power slice building block consists of three H-bridges, one for each output phase, and an isolation transformer. This power slice building block can be used to implement large SiC based MW power conversion systems

(from 4160V to 13.8 kV output voltages and up to 100 MW). The various voltage and power levels are achieved by series and parallel combinations of the power slices to fit a particular application. This method of scaling voltage and power in a modular design takes advantage of a rapid manufacturing and simplified testing process.

The AC/DC rectifier stage of each power cube can either be passive to suit most motor applications or can be an AFE stage, as describe previously, when needed for generation applications. With the active front end, the individual power cubes regulate their internal DC bus voltage and allow the drive as a whole to operate at the commanded power factors. This option can be useful in low short circuit duty applications where reactive power support can be generated to aid in stabilization of the system voltage at the point of interconnection.

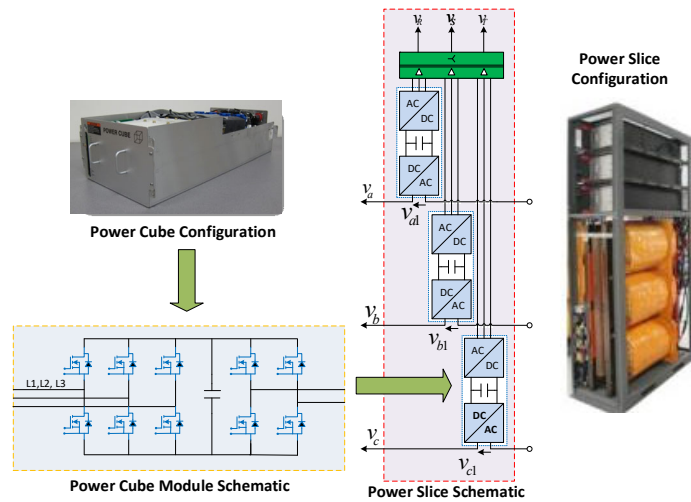


Figure 1: The general structure of the series connected full SiC H-bridge topology.

The multi-level synthesized output voltage is achieved with the use of the phase-shifted carrier PWM method [2]. The multi-level output decreases the voltage THD produced and reduces the dV/dt voltage stresses seen by the motor. Figure 2 illustrates example data and harmonic analysis given the standard Si IGBT based SCHB topology utilizing a 2 kHz and a 60 Hz fundamental. The system demonstrates excellent power quality with the output voltage THD below 2% up to 15 kHz with a relatively modest switching frequency.

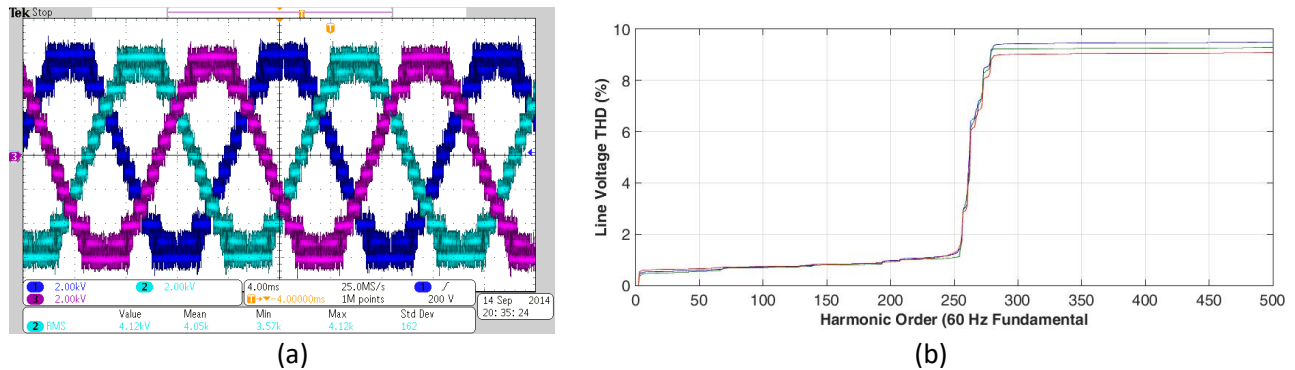


Figure 2: Measurements and harmonic analysis of the SCHB topology with a 4160V 60 Hz output voltage switching at 2 kHz; (a) scope capture of the output line to line voltage and (b) the percent output voltage THD calculations for the first 500th harmonics.

Using a 1.25MW and 4160V reference for the drive application, the semiconductor current rating is approximately 250A. Thanks to the relatively low H-bridge output voltage of the SCHB drive, 1700V or 1200V semiconductors can be used in three-slice and four-slice designs respectively. There are a number of commercially available devices in both 1700 V and 1200 V SiC MOSFET modules as well as 1700 V and 1200 V Si IGBT modules. Figure 3 demonstrates the operation of a hybrid SiC power cube utilizing SiC MOSFETs for the high frequency output and traditional Si IGBTs for the 60 Hz active front end.

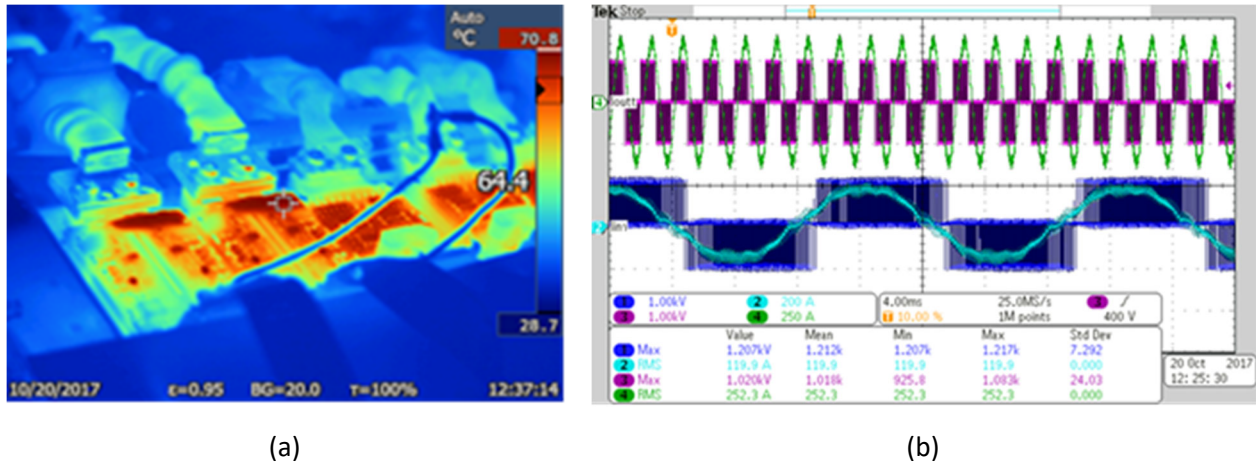


Figure 3: (a) Thermal imaging of the hybrid power cube undergoing initial full load testing and (b) the waveforms from the same hybrid power cube showing on the top the 500 Hz output voltage and currents and on the bottom, the voltage and current of one phase of the three phase active rectifier.

The primary advantage of WBG semiconductors over silicon technology is a reduction in switching loss which result from the high switching speeds and near zero recovery currents. This allows the switching frequency to be increased which is presently a limitation in high frequency, medium-voltage applications. One of the largest challenges of WBG semiconductors into a power converter system due to their electromagnetic compatibility concerns. High slew rates of the device voltage shall lead to excessive switching noise. For this reason, the layout and design of the SCHB drive with WBG semiconductors requires a high degree of understanding of potential pitfalls. Figure 4 demonstrates the benchtop testing of a second SiC MOSFET supplier and a solution to limiting the electromagnetic interference by utilizing a fiber optic gate driver interface (FGDI) board. The fiber optic link from the control system to the FGDI board is immune to electromagnetic interference and the very close proximity of the board to the gate driver limits any susceptibility to the electromagnetic interference created by the module switching.

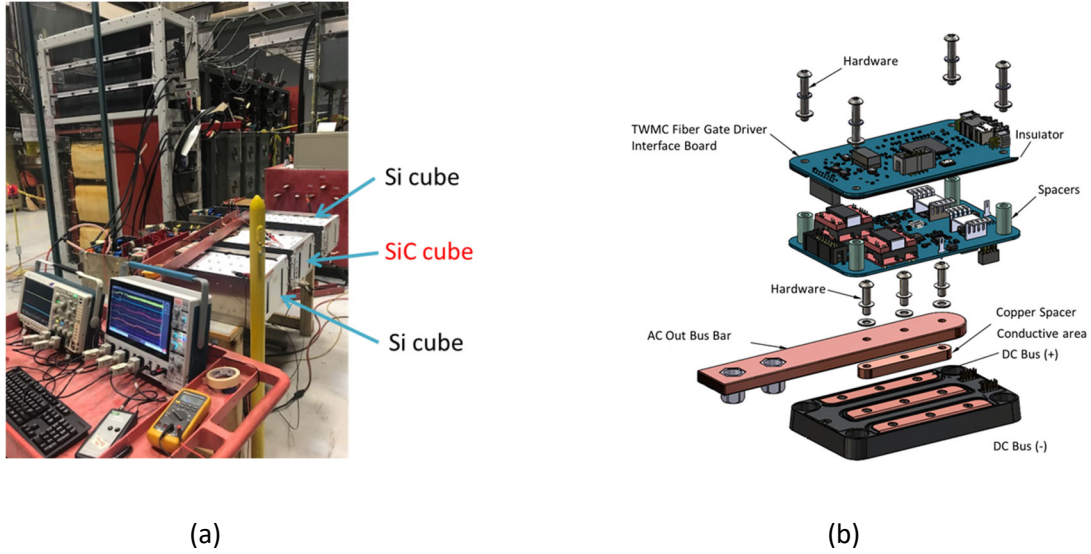


Figure 4: (a) Benchtop testing of the full SiC power cube and (b) the assembly of the SiC MOSFET, gate driver board and Fiber Optic Gate Driver Interface (FGDI) board used in the full SiC power cube design.

Specifications for a hybrid SiC medium voltage power converter at 1.2 MW reference design are provided in Table 1. For a full SiC MVD topology, the efficiency is expected to be over 98%. Key aspects of this technology implementation include very low inductance bus work design, gate driver optimization for desaturation protection, two-phase converter cooling implementation, and configurable medium voltage system insulation. Challenges included the overcoming of EMI issues when switching SiC devices at the converter input/output, management of switching losses to achieve required efficiency, and the overcoming of false desaturation protection trips.

Table 1: High Frequency Converter Specifications: Hybrid SiC System Topology

Specification	Value
Rated Real Power	1,200 kW
Rated Total Power	1,800 kVA
Input Voltage	4160 V
Output Voltage	4160 V
Output Current	250 A
Output Frequency	500 Hz
Switching Frequency	4 kHz Input / 6 kHz Output
Efficiency	96.4 %

3. High Speed Induction Machine

The specifications for the high-speed induction machine 1 MW reference design are given in Table 2 [3]. Figure 5 shows a prototype high speed induction machine with a flanged shaft prepared for factory acceptance tests. The high-speed induction machine design drivers are electromagnetic performance (torque/speed, torque pulsation), thermal management (losses, heat rejection), rotor-dynamic performance

(mode separation and excitation margins), rotor stress, motor insulation and coil design (high frequency operation) and bearing design (efficiency, heat rejection).

Table 2: High-Speed Induction Machine Specifications

Specification	Value
Rated Power	1,059 kW
Rated Speed	15,000 RPM
Nominal Voltage	4160 V
Nominal Current	235 A
Slip	0.0011
Efficiency	97 %



Figure 5: The prototype high speed induction machine with a flanged shaft prepared for factory acceptance tests.

For the high frequency applications, Litz or Roebel transposed wire is commonly used to minimize skin and proximity eddy effects. Because the wires usually have multiple strands, individually insulated and twisted to allow even current distribution among the strands, the wire's designed transposition reduces eddy current losses and improves the efficiency of the motor. The project team has developed and constructed stator windings using Litz wire previously for other applications, as shown in Figure 6, and has analyzed the power dissipation in the transposed cables with multiple strands.

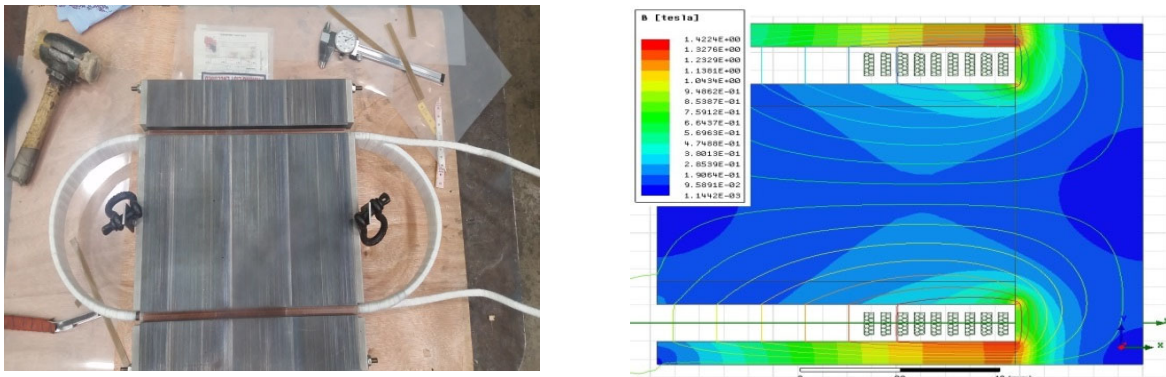
The use of Litz wire presents challenges to stator coil forming due to its extreme flexibility. This challenge also has an impact on the machine design. Coils made from Litz wire require additional processes and materials to stiffen the coil. At the same time, the material addition leads to poor heat transfer because of the added thermal resistance, so more cooling capacity is needed to remove the heat from the coils. Another concern using Litz wire is in the winding connections because each individual copper strand is coated with insulation. Insulation has to be removed using in-house developed methods before making the winding connections.



Figure 6: Litz wire coil sample, stator with Litz wire and Litz wire joint tests

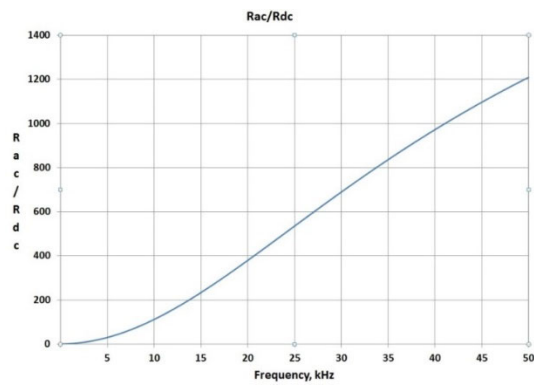
The Litz wire stator coil design has been shown to have higher than normal stator temperatures, thus requiring additional cooling. Figure 7 demonstrates the benchtop tester for the Litz wire coils, an electromagnetic simulation model of the Litz wire tester, and the ratio of the AC resistance to the DC resistance up to 50 kHz.

Unlike conventional copper strands, the transposed strands in Litz wire allow voids inside the stator slot, which has a negative impact on both the insulation and thermal design. Conduction cooling in the core section relies on intimate contact between copper, coil insulation and steel and excess voids in between the contacts can result in poor thermal conduction. Voids can also cause corona discharge due to the ionization of the gas inside the voids and, in combination with high temperatures, can cause insulation fatigue and breakdown.



(a)

(b)



(c)

Figure 7: (a) The benchtop tester for the Litz wire coils, (b) the electromagnetic simulation model of the Litz wire tester and (c) the ratio of the AC resistance to the DC resistance up to 50 kHz.

Bearing evaluation has a major impact on rotor-dynamics. Critical speed of a rotor is defined as when the rotor's rotational speed coincides with the rotor's natural frequency. Long hours of operation near critical speed can lead to component fatigue and mechanical failure. To shift rotor critical speed away from the operational speeds, one can adjust rotor geometry and bearing performance. Preliminary analysis using tilting pad bearings in Figure 8 shows a peak in the plot near 5,000 rpm, but none near the running speed (15,000 rpm). Also, based on the industry standard [4], the peak is not considered a critical speed because the amplification factor is less than 2.5 and is therefore considered critically damped. The final rotor design for this project used anti-friction bearings to minimize losses and squeeze film dampers to produce a critically damped response.

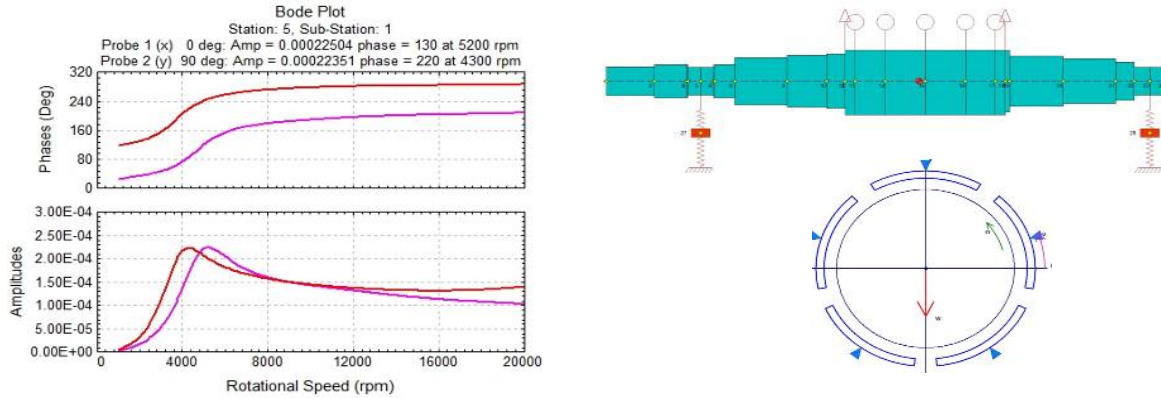
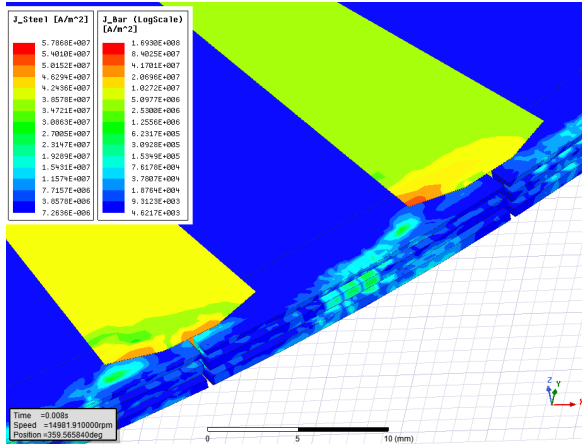


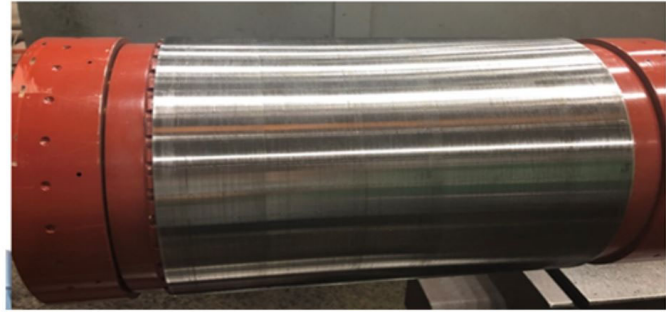
Figure 8: Bode plot (left) and rotor and bearing profile (right) used for the rotor dynamic design and analysis used in the high speed induction machine design.

The fundamental frequency for the high speed induction machine is 500 Hz. Since the machine is designed using 4 poles and 48 stator slots, the induced eddy currents on the rotor surface due to tooth ripple frequency with fundamental frequency of 12 kHz will be significant [5]. Therefore, slitting and grooving of the rotor surface to reduce induced eddy currents were studied to reduce the rotor eddy current losses [6]. It is concluded by performing several simulation studies that grooving of the rotor lamination surface is more effective than slitting. In addition, grooving depth is found more effective than width. Although greater depth and width reduce losses significantly, the final decision on the depth and width is made after an extensive trade-off study to retain the mechanical robustness of the rotor. After several 3D FEA runs, an optimum grooving design is finalized for the model as shown in Figure 9.

Validation tests between the un-grooved and grooved rotor were performed. By adding the grooves, the no load input power at the rated flux condition was reduced from 35.3 kW to 6.4 kW, a reduction of over 5.5 times. Because of the grooved surface, the friction and windage losses increased slightly.



(a)

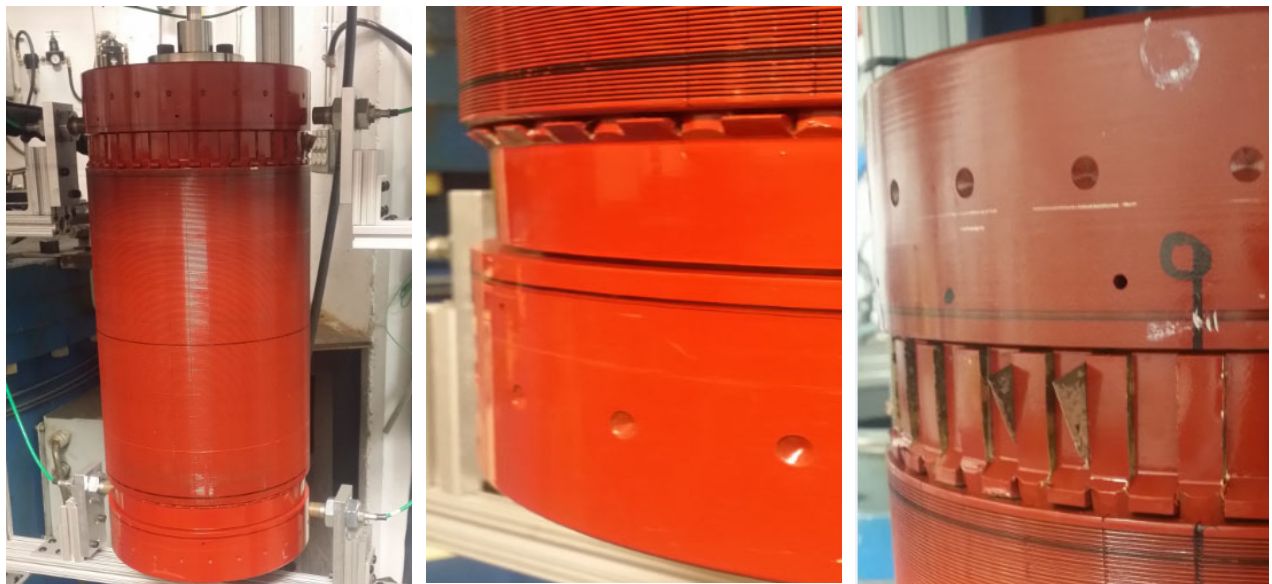


(b)

Figure 9: (a) FEA analysis of rotor grooving surface treatment to reduce eddy current losses on the induction machine rotor shown in (b) due to slot harmonics caused by the stator.

To validate the rotor design and manufacturing process, the rotor integrity was burst tested in an external facility. In the burst test, the rotor was subjected to rotational speeds up to 125% the rated speed (18,750 rpm) outside of the motor. These tests are used to evaluate the rotor integrity with regards to slot depth adjustments for improved power factor, shrink ring designs for better load distribution, circumferential rotor grooves for lower eddy current losses, and softer copper rotor bars to reduce cost and losses.

Figure 10 illustrates the successful results of the burst test on the rotor and the learnings provided by the test. The burst test exposed a manufacturing challenge associated with using manual torch brazing on the rotor bars. This was corrected in the final rotor design by utilizing an induction brazing process to ensure even heating and bonding around the entire rotor.



(a)

(b)

(c)

Figure 10: The burst test rotor with copper bars for higher efficiency and grooves to lower surface eddy currents. (a) Complete rotor after 25% over speed test, (b) lower rotor end rings showing no issues, and (c) upper rotor end rings showing some bar movement due to unreliable torch brazing that was corrected with induction brazing in the final rotor.

The high speed induction machine's initial design is Totally Enclosed, Water Cooled (TEWC). For this, an arrangement of two blowers and two air-to-water heat exchangers are affixed atop the stator. The blowers act to push air through the heat exchangers into the center of the stator. The hot air is then exhausted through both ends of the stator and back into the air boxes of the blowers. In this application, the blowers are controlled by variable frequency drives to enable higher efficiencies across all the operating ranges of the induction machine.

Figure 11 demonstrates the FEA thermal analysis that was performed on the high-speed induction machine to analyze the complete motor heat transfer paths and determine the anticipated temperature rises on the stator and rotor. Several different air flow rates were modeled and tradeoffs between temperature rise, efficiency and windage losses were studied. The thermal analysis was fed back into the electromagnetic design to determine the final efficiency of the machine.

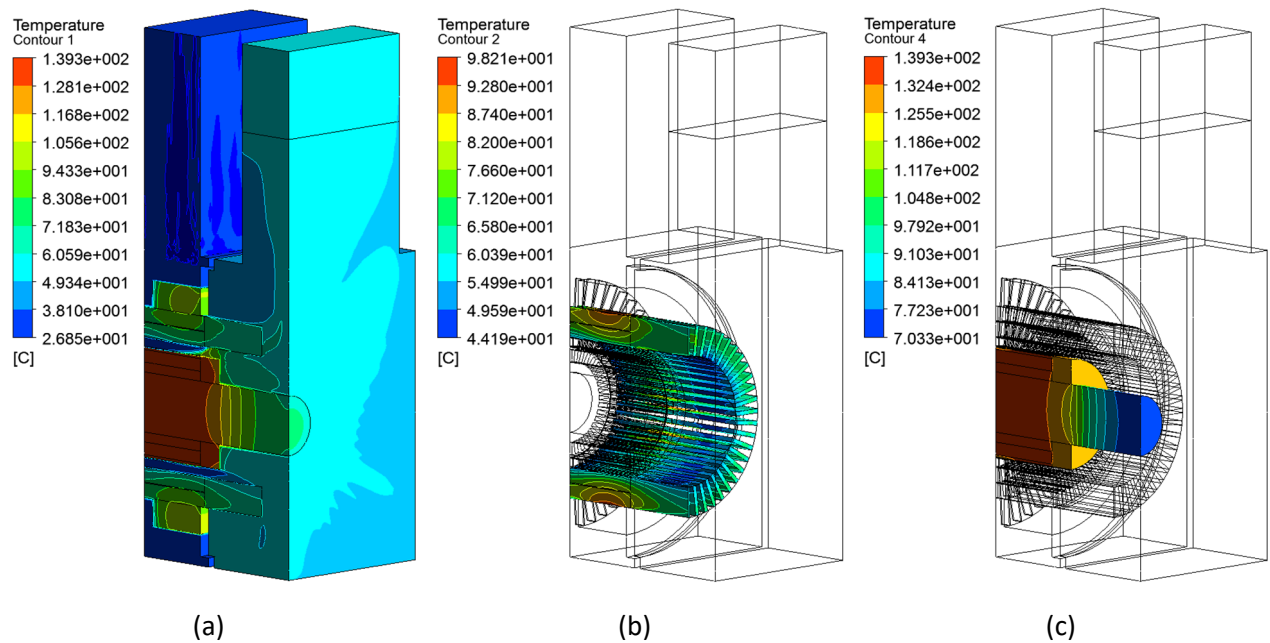


Figure 11: FEA thermal analysis of the induction machine for forced air cooling with a flow rate of 2400 CFM of the (a) full induction machine model, (b) stator core, and (c) rotor.

4. Fully Integrated System Validation

To validate the fully integrated system consisting of the high-speed induction machine and high frequency medium voltage power converter, a high-speed bi-directional dynamometer has been developed at Clemson University's eGRID Center. Figure 12 illustrates the validation setup including the fully integrated system, a high-speed gearbox and a low speed motor. The high-speed gearbox has a gear ratio of 15,000/1,800 which allows for the dynamometer to test up to speeds in excess of 20,000 RPM using a conventional induction machine. The low speed motor is connected to a bi-directional SCHB motor drive that allows the complete system to be tested up to full speed and full power in both motoring and generation modes. This enables the complete validation of the high-speed induction machine in terms of electromagnetic, thermal, and dynamic performance.

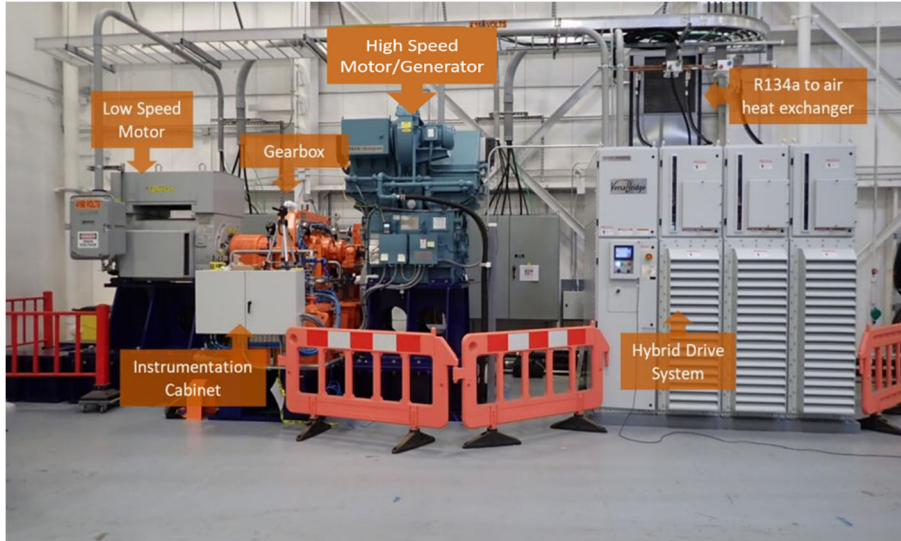


Figure 12: The high-speed dynamometer test setup for system validation at the Clemson University eGRID Center.

Additionally, the grid side connection of the high frequency medium voltage power converter is connected directly to the eGRID Center’s power amplifier units that are proven for full scale type testing and validating the grid integration compliance of Distributed Energy Resources (DER), such as wind turbines, solar inverters and battery energy storage systems.

The project team was able to complete two full and one half power heat run of the system to determine the efficiency of the high-speed motor, high frequency variable speed drive, and the system as a whole. The test ran for 2 hours before the bearing and winding temperatures stabilized. Tables 3 and 4 demonstrate the measured power and efficiency values.

Table 3: Full rated power motoring heat run results

Real Power (kW)			Efficiency		
Drive Input	Drive Output	Shaft	Drive	HSM	System
1084.8	1045.1	993.8	96.3%	95.1%	91.6%
1088.2	1056.6	987.8	97.1%	93.5%	90.8%

Table 4: Half rated power motoring heat run results

Real Power (kW)			Efficiency		
Drive Input	Drive Output	Shaft	Drive	HSM	System
577.7	557.7	501.5	96.5%	90.1%	86.8%

The real power values reported are the average of 60 values over a one-minute window and the efficiencies are calculated from the real power values. DOE FOA target system efficiency was 93% at full load and 90% at half load.

Figure 13 shows the high-speed induction machine torque, speed, vibration and winding temperature data. Overall, the winding temperature was well within the design limits of the machine and below 100 C

at all locations. The bearing temperatures were also below 100 C for the complete heat run. Figure 14 provides the parameters of the water cooling of the TEWC motor and the air temperatures within the blower air boxes and end turns of the machine.

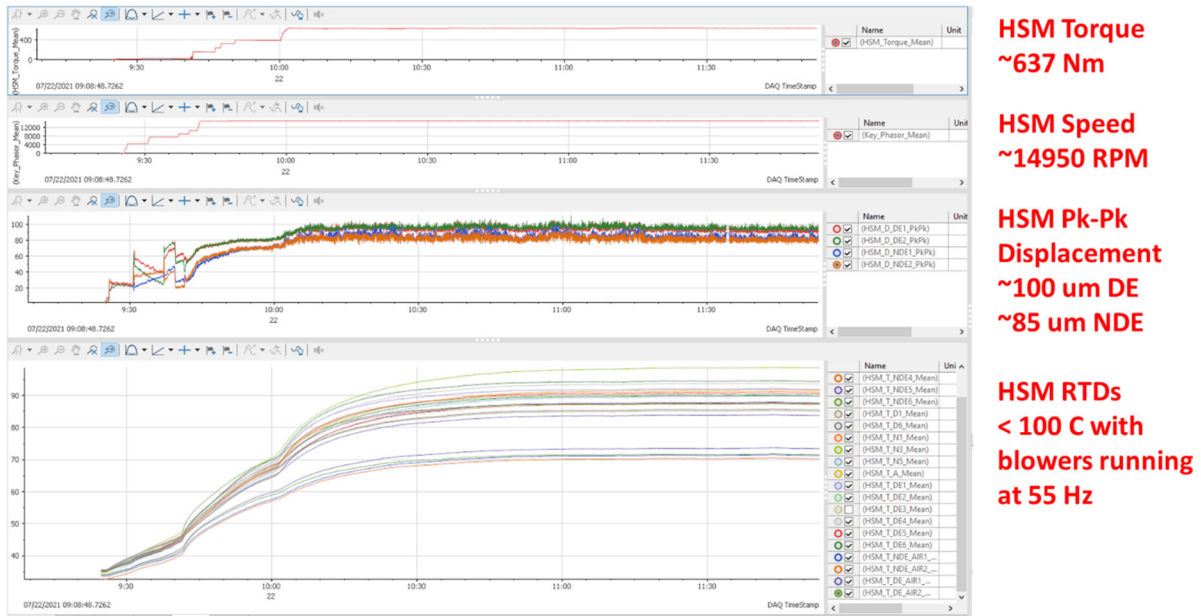


Figure 13: 100% Power Heat Run Data: High Speed Machine Torque, Speed, Vibration and Winding Temperatures.

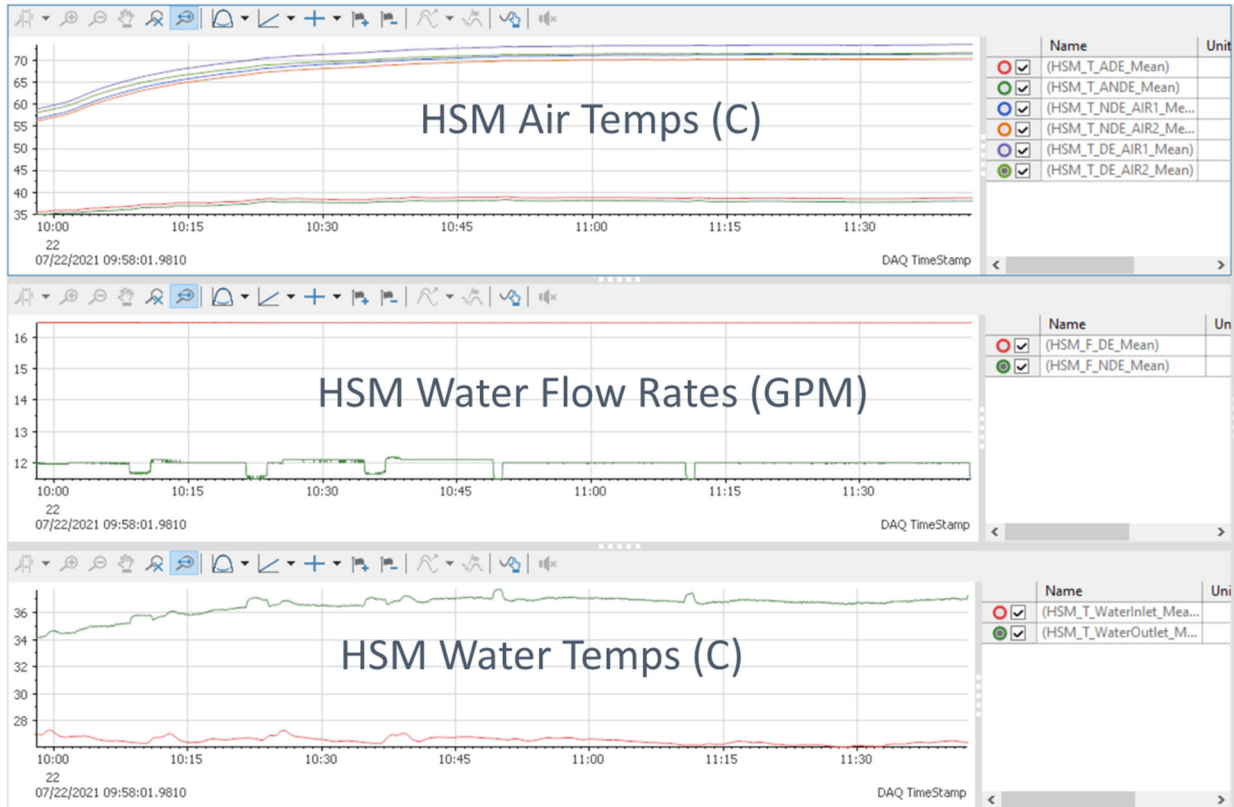
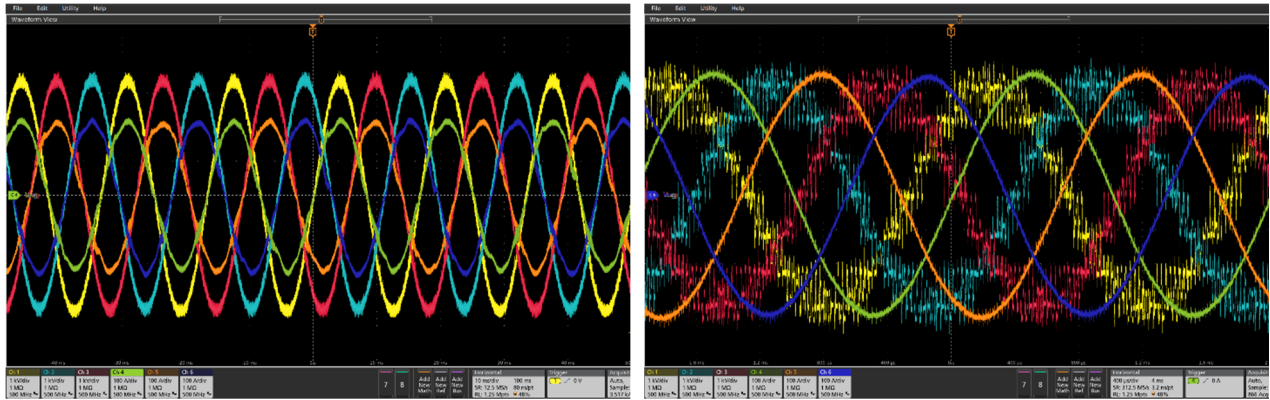


Figure 14: 100% Power Heat Run Data: High Speed Machine Cooling System Data.

Figure 15 illustrates the drive input and output voltage and currents for 100% power run. Figures 16 and 17 shows FFT analysis of these voltages and currents. Table 5 lists THD calculated based on FFT analysis.



(a) Input Voltage and Current

(b) Output Voltage and Current

Figure 15: Input and output voltage and current waveform for 100% power heat run.

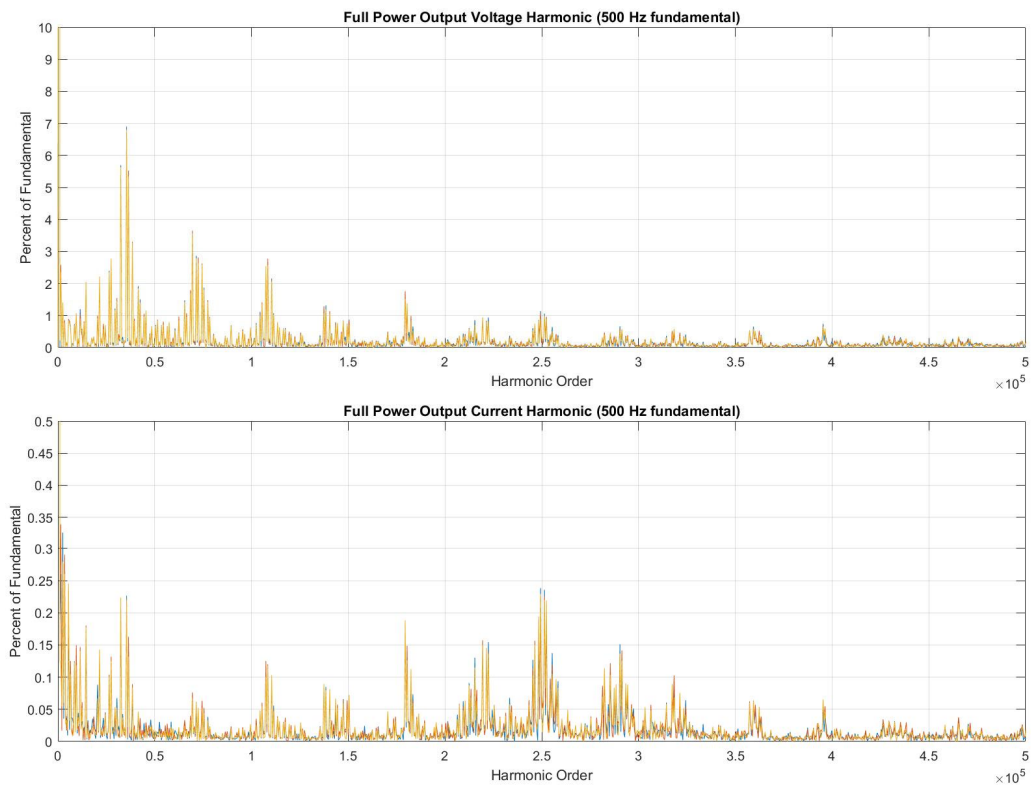


Figure 16: Output harmonics data for 100% power heat run.

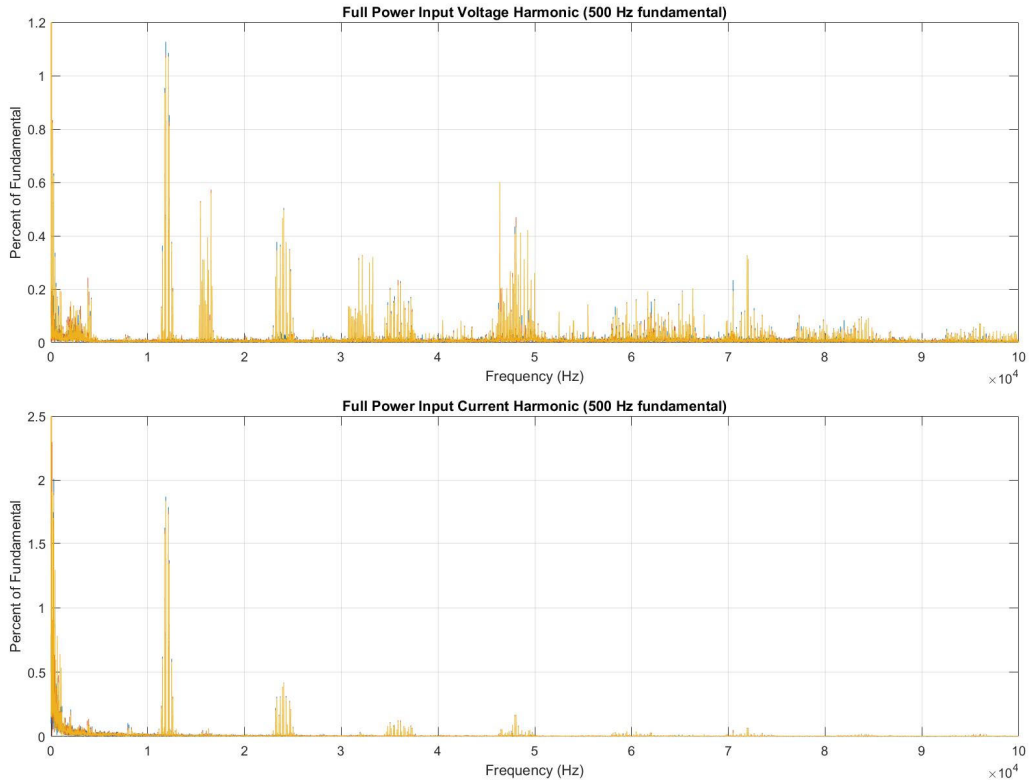


Figure 17: input harmonics data for 100% power heat run.

Table 5: THD for input and output drive voltage and current for 100% power test.

	Voltage THD		Current THD	
Input	V_{ug}	3.88%	I_u	5.95%
	V_{vg}	3.83%	I_v	5.98%
	V_{wg}	3.86%	I_w	5.90%
Output	V_{ug}	5.0%	I_u	0.67%
	V_{vg}	5.1%	I_v	0.71%
	V_{wg}	5.0%	I_w	0.61%

5. Other Product

5.1. Patents

- H. Karmaker, E. Chen, J. Keck and P. Guedes-Pinto, “High Speed Induction Machine”, US Patent Application 16/227,639 dated 12/20/2018.
- E. Ledezma, P. Guedes-Pinto, R. Pipho, B. Palle, R. Edwards, A. Skorcz, “High Frequency Medium Voltage Drive System for High Speed Machine Applications”, US Patent Application 16/205,879 dated 11/30/2018.
- E. Ledezma, B. Palle, R. Edwards, R. Metzler, “Cooling Methods for Medium Voltage Drive Systems”, US Patent Application 16/205,840 dated 11/30/2018.

5.2. Papers

- H. Karmaker, P. Guedes-Pinto, E. Chen, J. Keck, E. Ledezma J. Leonard, and J. Fox, “High Speed MW-rated induction motor drive system”, Presented at IEEE International Electric Machine and Drive Conference (IEMDC), Miami, FL, May 2017.
- D. Millare, R. Hadidi, M. H. McKinney, J. Leonard, and J. C. Fox, "Calculations for Asymmetrical Fault Synthesis for Evaluating Ride-Through of Grid Connected Solar Inverters," 9th IEEE International Symposium on Power Electronics for Distributed Generation Systems (PEDG), Charlotte, NC, June 2018.
- E. Ledezma, D. Sarandria, S. Ahsani, H. Karmaker, J. Fox, J. Leonard, and T. King, “SiC Based MVD Power Technology for Heat Recovery Applications”, Presented at Gas Machinery Conference, Louisville, Ky, October 2021.

5.3. Presentations

- TECO Westinghouse Motor Company and Clemson University hosted DOE Project Update meetings to review overall progress of the project.
- H. Karmaker presented a paper on “High Speed MW-rated induction motor drive system at the IEEE International Electric Machine and Drive Conference (IEMDC), Miami, FL, May 2017.
- J. Fox presented a paper on “SiC Based MVD Power Technology for Heat Recovery Applications” at Gas Machinery Conference, Louisville, Ky, October.

5.4. Reports

- Three invention disclosure reports (EERE 357) were submitted in December of 2018.
- Quarterly technical progress reports were submitted by TWMC and Clemson University teams.

6. Impacts

The project enhanced manufacturing capabilities within the United States by developing innovative processes and systems including developed Litz wire stator coil assemblies, rotor containment, squeeze film damper, and manufacturing processes for high speed applications. TECO Westinghouse Motor Company has compiled a list of potential end users and original equipment manufacturers (OEMs) that would be interested in the high speed motor and drive system. These parties cover the chemical, refining and general industry markets. TWMC will obtain from these parties their specification requirements and operational preferences, as well as cost and lead-time requirements. TWMC and Clemson are also evaluating trade-shows, conferences and user group meetings to attend in order to increase the awareness of the project and its goals. TWMC is also in the process of building a second machine to investigate heat recovery applications using the system as a high speed generator [7].

7. References

- [1] Ledezma, E., et. al., "Development of a modular configurable multi-megawatt power amplifier," Industrial Electronics Society, IECON 2013 - 39th Annual Conference of the IEEE , vol., no., pp.631,636, 10-13 Nov. 2013.
- [2] Holmes, D. G., Lipo, T., Pulse Width Modulation for Power Converters: Principles and Practice, IEEE Press, 2003.
- [3] Karmaker, H., et. al., "High speed MW-rated induction motor drive system," 2017 IEEE International Electric Machines and Drives Conference(IEMDC), Annual Conference of the IEEE, May, 2017.
- [4] ANSI/API Standard 541 4th edition 2004.
- [5] J. Greig and E. Freeman, "Simplified presentation of eddy current loss equation for laminated pole shoes", Proc. IEE, 1963.
- [6] Y. Gessese, A. Binder and B. Funieru, "Analysis of the effect of radial rotor surface grooves on rotor losses of high speed solid rotor induction motor," SPEEDAM 2010.
- [7] Ledezma, E. et. al., "SiC Based MVD Power Technology for Heat Recovery Applications," Presented at Gas Machinery Conference, Louisville, Ky, October 2021.